

Hypersensitivity to perturbations of quantum-chaotic wave-packet dynamics

P. G. Silvestrov,^{1,2} J. Tworzydło,^{1,3} and C. W. J. Beenakker¹

¹*Instituut-Lorentz, Universiteit Leiden, P.O. Box 9506, 2300 RA Leiden, The Netherlands*

²*Budker Institute of Nuclear Physics, 630090 Novosibirsk, Russia*

³*Institute of Theoretical Physics, Warsaw University, Hoza 69, 00-681 Warszawa, Poland*

(Dated: 30 June 2002)

We re-examine the problem of the “Loschmidt echo”, which measures the sensitivity to perturbation of quantum chaotic dynamics. The overlap squared $M(t)$ of two wave packets evolving under slightly different Hamiltonians is shown to have the double-exponential initial decay $\propto \exp(-\text{constant} \times e^{2\lambda_0 t})$ in the main part of phase space. The coefficient λ_0 is the self-averaging Lyapunov exponent. The average decay $\overline{M} \propto e^{-\lambda_1 t}$ is single exponential with a different coefficient λ_1 . The volume of phase space that contributes to \overline{M} vanishes in the classical limit $\hbar \rightarrow 0$ for times less than the Ehrenfest time $\tau_E = \frac{1}{2}\lambda_0^{-1}|\ln \hbar|$. It is only after the Ehrenfest time that the average decay is representative for a typical initial condition.

PACS numbers: 05.45.Mt, 03.65.Sq, 03.65.Yz, 05.45.Pq

Chaos in classical mechanics is characterised by an exponential sensitivity to initial conditions: The separation of two trajectories that are initially close together increases in time $\propto e^{\lambda t}$ with a rate given by the Lyapunov exponent λ . There is no such sensitivity in quantum mechanics, because the overlap of two wave functions is time independent. This elementary observation is at the origin of a large literature (reviewed in a textbook [1]) on quantum characterisations of chaotic dynamics.

One particularly fruitful line of research goes back to the proposal of Schack and Caves [2], motivated by earlier work of Peres [3], to characterise chaos by the sensitivity to perturbations. Indeed, if one and the same state ψ_0 evolves under the action of two different Hamiltonians H and $H + \delta H$, then the overlap

$$M(t) = |\langle \psi_0 | e^{i(H+\delta H)t/\hbar} e^{-iHt/\hbar} | \psi_0 \rangle|^2 \quad (1)$$

is not constrained by unitarity. Jalabert and Pastawski [4] discovered that $M(t)$ (which they referred to as the “Loschmidt echo”) decays $\propto e^{-\lambda t}$ if ψ_0 is a narrow wave packet in a chaotic region of phase space, providing an appealing connection between classical and quantum chaos.

The discovery of Jalabert and Pastawski gave a new impetus [5] to what Schack and Caves called “hypersensitivity to perturbations” of quantum chaotic dynamics. The present paper differs from this body of literature in that we consider the *statistics* of $M(t)$ as ψ_0 varies over the chaotic phase space. We find that the average decay $\overline{M}(t) \propto e^{-\lambda t}$ is due to regions of phase space that become vanishingly small in the classical limit $\hbar_{\text{eff}} \rightarrow 0$. (The effective Planck constant $\hbar_{\text{eff}} = \hbar/S_0$ is set by the inverse of a typical action S_0 .) The dominant decay is a *double* exponential $\propto \exp(-\text{constant} \times e^{2\lambda t})$, so it is truly “hypersensitive”. The slower single exponential decay is recovered at the Ehrenfest time $\tau_E = \frac{1}{2}\lambda^{-1}|\ln \hbar_{\text{eff}}|$.

Before presenting our analytical theory we show in Fig. 1 the data from a numerical simulation that illustrates the hypersensitivity mentioned above. The Hamil-

tonian is the quantum kicked rotator [1]

$$H = \frac{\hat{p}^2}{2} + K \cos x \sum_n \delta(t - n), \quad \hat{p} = \frac{\hbar}{i} \frac{d}{dx}. \quad (2)$$

The perturbed Hamiltonian $H' = H + \delta H$ is obtained by the replacement $K \rightarrow K + \delta K$. The coordinate x is periodic, $x \equiv x + 2\pi$. To work with a finite dimensional Hilbert space we discretize $x_k = 2\pi k/N$, $k = 1, 2, \dots, N$. The momentum $p_m = m\hbar$ is a multiple of \hbar , to ensure single-valued wavefunctions. For $\hbar \equiv \hbar_{\text{eff}} = 2\pi/N$ the restriction to the first Brillouin zone results in a single band $p_m = 2\pi m/N$, $m = 1, 2, \dots, N$. The time evolution $e^{-iHn/\hbar} \equiv U^n$ after n periods, of the initial Gaussian wave packet $\psi_k = N^{-1/2} \exp(\pi N^{-1}[2im_0k - (k - k_0)^2])$, is given by the Floquet operator in the x -representation:

$$U_{k'k} = \frac{1}{\sqrt{N}} \exp\left(\frac{i\pi(k' - k)^2}{N} - i\frac{NK}{2\pi} \cos \frac{2\pi k}{N}\right). \quad (3)$$

We use the fast Fourier transform algorithm to compute U^n for N up to 10^6 [6].

We study the statistics of $M(t)$ by comparing in Fig. 1 three different ways of averaging over initial positions (m_0, k_0) of the Gaussian wave packet. We used $K = 10$, $\delta K = 1.6 \cdot 10^{-3}$ and $N = 10^6$ ($\hbar_{\text{eff}} = 6.28 \cdot 10^{-6}$). While the average \overline{M} decays exponentially, the two logarithmic averages have a much more rapid initial decay. We estimate that $M < 10^{-23}$ at $n = 3$ for about 30% of randomly chosen initial conditions. For the same point $n = 3$ only 9% of initial conditions (corresponding to $M > 0.2$) account for 80% of the total value of \overline{M} . The typical decay of $M(t)$ is therefore much more rapid than the exponential decay of the average \overline{M} .

Statistical fluctuations also affect the decay rate of \overline{M} , set by the Lyapunov exponent according to Ref. [4]. The definition of the Lyapunov exponent $\lambda_0 = \lim_{t \rightarrow \infty} t^{-1} \ln |\delta x(t)/\delta x(0)|$ gives $\lambda_0 = 1.65$ for the classical kicked rotator with $K = 10$. However, $\overline{M}(t)$ in Fig. 1 has exponent $\lambda_1 = 1.1$, defined by

$$\lambda_j = - \lim_{t \rightarrow \infty} (jt)^{-1} \ln |\overline{\delta x(t)/\delta x(0)}|^{-j}. \quad (4)$$

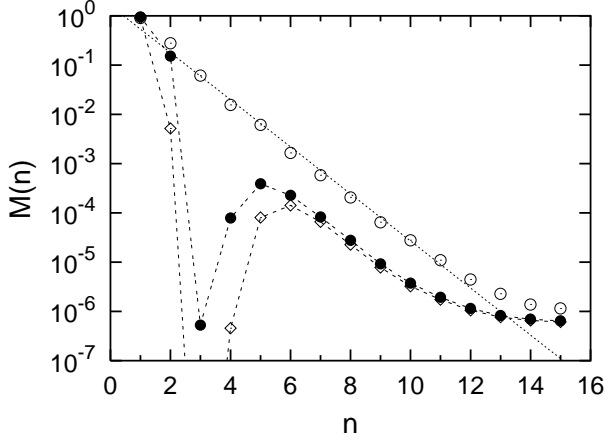


FIG. 1: The overlap M at $t = n$ for the quantum kicked rotator for three different ways of averaging: $\circ \bar{M}$, $\diamond \exp(\ln \bar{M})$, $\bullet \exp[-\exp(\ln(-\ln \bar{M}))]$. We took $K = 10$, $\delta K = 1.6 \cdot 10^{-3}$, $N = 10^6$. Averages are taken over 2000 random initial conditions of a Gaussian wave packet. The dotted line shows the Lyapunov decay $\propto e^{-n\lambda_1}$ with $\lambda_1 = 1.1$. At $n = 3$ we have only an upper bound for the logarithmic averages because cancelations in the calculation limit the accuracy.

Since fluctuations of $t^{-1} \ln |\delta x(t)/\delta x(0)|$ decrease like $t^{-1/2}$ the Lyapunov exponent λ_0 is self-averaging [7], while the λ_j 's are not.

For an analytical description we start from the Gaussian one-dimensional wave packet

$$\psi(x) = \left(\frac{\alpha}{\pi\hbar}\right)^{1/4} \exp\left(i\frac{p_0 x}{\hbar} + (i\beta - \alpha)\frac{(x - x_0)^2}{2\hbar}\right). \quad (5)$$

The wave packet is centered at the point $x_0(t), p_0(t)$ which moves along a classical trajectory. Initially $\beta(t=0) = 0$ and $\alpha(t=0) = 1$. Divergence of trajectories leads to the exponential broadening of the packet, thus $\alpha(t) \propto \exp(-2\lambda t)$. Since $\alpha \ll 1$ for $t \gg 1/\lambda$, the wave packet in phase space becomes highly elongated with length $l_{\parallel} = \sqrt{\hbar(1 + \beta^2)}/\alpha$ and width $l_{\perp} = \hbar/l_{\parallel}$. The parameter $\beta = \Delta p/\Delta x$ represents the tilt angle of the elongated wave packet [8]. The Gaussian approximation (5) breaks down at the Ehrenfest time $\tau_E = \frac{1}{2}\lambda^{-1}|\ln \hbar|$, when l_{\parallel} becomes of the order of the size of the system.

We assume that ψ evolves according to Hamiltonian $H(K)$ and ψ' according to $H' = H(K + \delta K)$. The overlap $M = |\langle \psi' | \psi \rangle|^2$ of the two Gaussian wave packets is

$$M = \sqrt{\frac{\alpha\alpha'}{\bar{\alpha}^2 + 4\delta\beta^2}} \exp\left(-\frac{\bar{\alpha}(\delta p - \bar{\beta}\delta x)^2}{2(\bar{\alpha}^2 + 4\delta\beta^2)\hbar} - \frac{\alpha\alpha'\delta x^2}{2\alpha\hbar}\right), \quad (6)$$

in terms of the (weighted) mean $\bar{\alpha} = (\alpha + \alpha')/2$, $\bar{\beta} = (\beta'\alpha + \beta\alpha')/(\alpha + \alpha')$ and difference $\delta p = p'_0 - p_0$, $\delta x = x'_0 - x_0$, $\delta\alpha = \alpha' - \alpha$, $\delta\beta = \beta' - \beta$. In order of magnitude, $\delta\beta/\bar{\beta} \simeq \delta\alpha/\bar{\alpha} \simeq \delta K \ll 1$. The displacement vector $(\delta x, \delta p)$ has component $\Delta_{\parallel} \simeq \delta K e^{\lambda t}$ parallel to the elongated wave packets and component $\Delta_{\perp} \simeq \delta K$ perpendicular to them (see Fig. 2).

Depending on the strength of perturbation one may distinguish three main regimes: $\delta K < \hbar$, $\hbar < \delta K < \sqrt{\hbar}$, and $\delta K > \sqrt{\hbar}$. We will consider in detail the intermediate regime $\hbar < \delta K < \sqrt{\hbar}$ and discuss the two other regimes more briefly at the end of the paper. (The simulations of Fig. 1 are at the upper end of the intermediate regime, since $\delta K = 1.6 \cdot 10^{-3}$ and $\sqrt{\hbar} = 2.5 \cdot 10^{-3}$.) The three regimes may be characterised by the relative magnitude of the Ehrenfest time τ_E and the perturbation dependent time scale $\tau_0 = \frac{1}{2}\lambda^{-1}|\ln \delta K|$. In the intermediate regime one has $\frac{1}{2}\tau_E < \tau_0 < \tau_E$.

To estimate the relative magnitude of the two terms in the exponent of Eq. (6) we write

$$\delta p - \bar{\beta}\delta x = (1 + \bar{\beta}^2)^{1/2}\Delta_{\perp} = f\delta K, \quad (7)$$

$$\frac{\bar{\alpha}}{\bar{\alpha}^2 + 4\delta\beta^2} \equiv Q = \frac{e^{2\lambda t}}{1 + (ge^{2\lambda t}\delta K)^2}. \quad (8)$$

Here f and g are functions of order unity of time t and the initial location x_i, p_i of the wave packet. The second term in the exponent (6) is of order $\bar{\alpha}\delta x^2/\hbar \simeq \delta K^2/\hbar$, while the first term is of order $Q\delta K^2/\hbar$. Since $Q \gg 1$ for $t < 2\tau_0$, and since $2\tau_0 > \tau_E$ in the intermediate regime, we may neglect the second term relative to the first term within the entire range $t < \tau_E$ of validity of the Gaussian approximation. Eq. (6) thus simplifies to

$$M = (\bar{\alpha}Q)^{1/2} \exp\left[-\frac{1}{2}Q(f\delta K)^2/\hbar\right]. \quad (9)$$

We seek the statistics of $M(t)$ generated by varying x_i, p_i . The statistics is non-trivial because fluctuations in f of order unity cause exponentially large fluctuations in M if $Q\delta K^2/\hbar \gg 1$, which is the case for $2\tau_0 - \tau_E < t < \tau_E$. The average of M is then dominated by the nodal lines $x_n(p)$ in phase space at which f vanishes (at a particular time t). If Δx_n is the typical spacing of these lines at constant p , then the derivative $\partial f/\partial x_i$ at x_n is of order $1/\Delta x_n$. This yields

$$\begin{aligned} \bar{M} &= (\bar{\alpha}Q)^{1/2} \int \frac{dx}{\Delta x_n} \exp\left[-\left(\frac{x - x_n}{\Delta x_n}\right)^2 \frac{Q\delta K^2}{2\hbar}\right] \\ &\simeq (\bar{\alpha}\hbar/\delta K^2)^{1/2} = (\sqrt{\hbar}/\delta K)e^{-\lambda t}. \end{aligned} \quad (10)$$

Assuming independent fluctuations in the (perturbation dependent) distribution of nodal lines and in the rate of divergence of trajectories for the individual Hamiltonian, we incorporate fluctuations in λ in Eq. (10) via $\exp(-\lambda t) \rightarrow \exp(-\lambda_1 t)$, in accordance with (4). Hence we recover the exponential decay of the Loschmidt echo [4], although with the exponent λ_1 instead of λ_0 (in agreement with the numerics of Fig. 1). The exponential decay sets in for $t > 2\tau_0 - \tau_E$, while for shorter times \bar{M} remains close to unity [9].

The volume \mathcal{V} of phase space near the nodal lines contributing to \bar{M} is of order $\mathcal{V} = (\hbar/Q\delta K^2)^{1/2}$. This volume decreases exponentially in time for $t < \tau_0$, reaching the minimal value $\mathcal{V}_0 = \sqrt{\hbar}/\delta K \ll 1$ at τ_0 . For larger

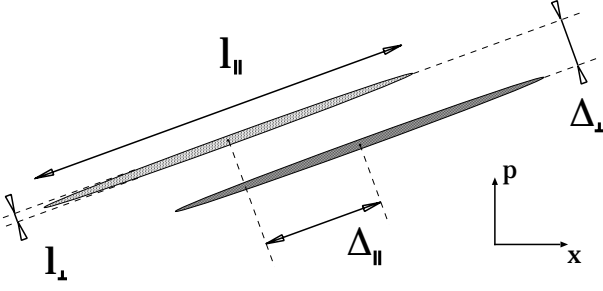


FIG. 2: Schematic illustration of two perturbed wave packets in phase space for $t < \tau_0$.

times \mathcal{V} increases, saturating at a value of order unity at τ_E . We therefore conclude that the average \overline{M} is only representative for the typical decay if $t > \tau_E$. For smaller times the average is dominated by rare fluctuations that represent only a small fraction of the chaotic phase space.

To obtain an average quantity that is representative for a typical point in phase space we take logarithmic averages of Eq. (9). For $t < \tau_0$ one has

$$\ln \overline{M} \simeq -(\delta K^2/\hbar) \exp(2\lambda_{-2}t), \quad (11)$$

$$\ln \ln(1/\overline{M}) = 2\lambda_0 t - \ln(\hbar/\delta K^2) + \mathcal{O}(1). \quad (12)$$

(The coefficient λ_{-2} in $\ln \overline{M}$ appears because we average the square of displacement.) The double logarithmic average (12), given by the self-averaging Lyapunov exponent λ_0 , is least sensitive to fluctuations and is representative for the main part of phase space. The typical overlap thus has the double-exponential decay

$$M \simeq \exp(-\text{constant} \times (\delta K^2/\hbar) e^{2\lambda_0 t}), \quad (13)$$

down to a minimal value $M_0 \simeq \exp(-\delta K/\hbar)$ at $t = \tau_0$.

The initial decay (13) for $t \ll \tau_0$ is the same as obtained in Ref. [10] for the classical fidelity (defined as the overlap of two classical phase space densities). In that problem the role of \hbar is played by the initially occupied volume of phase space. A superexponential decay of the classical fidelity has also been obtained by Eckhardt [11].

The origin of the decay (13) is illustrated in Fig. 2. For $t < \tau_0$ the wave packets are nearly parallel ($\delta\beta \ll \overline{\alpha}$), displaced laterally by an amount $\Delta_\perp \propto \delta K$. Their overlap is an exponential function $\propto \exp(-\Delta_\perp^2/l_\perp^2)$, where the width l_\perp of each wave packet decreases exponentially in time $\propto e^{-\lambda t}$. Hence the double-exponential decay.

For $t > \tau_0$ (when $\delta\beta \gg \overline{\alpha}$) the overlap of the two wave packets is dominated by their crossing point x_c, p_c . The overlap $M \simeq \exp(-\text{constant} \times |x_c - x_0|^2/l_\parallel^2)$ now increases with time, because $l_\parallel \propto e^{\lambda t}$. Since $|x_c - x_0| \simeq \Delta_\perp/\delta\beta \simeq f$, the crossing point falls outside of the range of validity of the Gaussian approximation unless $|f| \ll 1$. The result (10) is justified (because it is dominated by nodes of f), but we can not use the Gaussian approximation to extend the formula (13) for the typical decay to $t > \tau_0$. The typical decay and the average decay become the same at τ_E ,

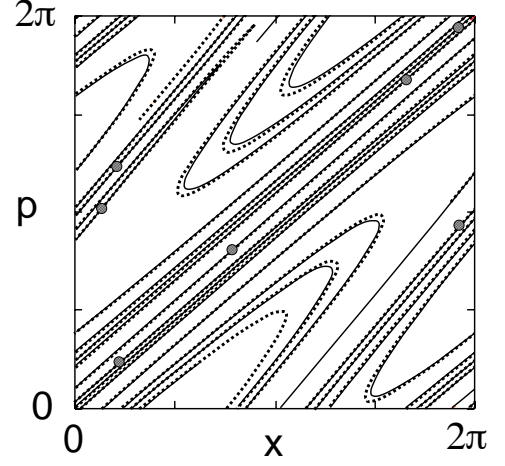


FIG. 3: Two perturbed wave packets in phase space for $\tau_E < t < \tau_E + 2\tau_0$. The lines show $p(x)$ (solid) and $p'(x)$ (dashed) extracted from the Husimi function evolved with the quantum kicked rotator, for $N = 10^6$, $K = 7$, $\delta K = 0.1$, $n = 5$. Dots show the crossing points x_j that contribute to the overlap in stationary phase approximation.

so the typical M should increase from its minimal value M_0 at τ_0 to the value $M_E = (\sqrt{\hbar}/\delta K)e^{-\lambda\tau_E} = \hbar/\delta K$ at τ_E . Both M_0 and M_E are $\ll 1$, but M_0 is exponentially small in $\delta K/\hbar$ while M_E is only algebraically small.

For $t > \tau_E$ one can use the semiclassical WKB description of elongated wave packets, along the lines of Refs. [12]. The phase space representation of the wave function ψ is concentrated along the line on the torus $p(x)$ of length $l_\parallel \simeq \sqrt{\hbar}e^{\lambda t} \gg 1$, see Fig. 3. The function $p(x)$ is multivalued and each branch k has a WKB wave function with amplitude $\rho_k \approx 1/l_\parallel$ and phase σ_k :

$$\psi = \sum_k \sqrt{\rho_k} e^{i\sigma_k/\hbar}, \quad p_k = d\sigma_k/dx. \quad (14)$$

For $\delta K > \hbar$ the overlap of two oscillating wave functions ψ, ψ' of the form (14) may be found in stationary phase approximation. The stationary points are given by the crossings $p(x_j) = p'(x_j)$ of the two lines $p(x), p'(x)$ given by the evolution with Hamiltonians H, H' . For $\tau_E < t < \tau_E + 2\tau_0$ the number of crossings N_c is proportional to l_\parallel and independent of δK . This is because both the lateral displacement of p and p' and their relative angle are of the same order δK . (In Fig. 3 we have $l_\parallel \simeq 20N_c$.) Each crossing contributes to $\langle \psi|\psi' \rangle$ an amount

$$P_j = \sqrt{\rho(x_j)\rho'(x_j)} \int dx \exp \left[i \frac{\kappa(x - x_j)^2}{2\hbar} + i\phi_j \right] \simeq (e^{i\phi_j}/l_\parallel) \sqrt{\hbar/\delta K}, \quad (15)$$

where $\kappa = d^2(\sigma - \sigma')/dx^2|_{x_j} \simeq \delta K$ and $\hbar\phi_j = \sigma(x_j) - \sigma'(x_j)$. The phase ϕ_j varies randomly from one crossing

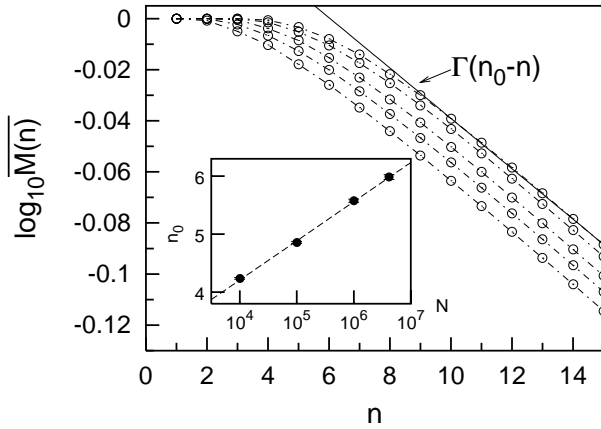


FIG. 4: Decay of the average overlap for the quantum kicked rotator ($K = 10$) in the golden-rule regime. We keep $\Gamma = 0.023(N\delta K)^2$ fixed by taking $\delta K \equiv 1/N$. Circles from bottom to top give \bar{M} for $N = 10^3, 10^4, 10^5, 10^6, 4 \cdot 10^6$. The inset demonstrates that n_0 scales with $\log N$, as expected for the Ehrenfest time.

to the other, leading to

$$\bar{M} = \frac{\hbar}{l_{\parallel}^2 \delta K} \sum_{j,j'=1}^{N_c} \overline{e^{i(\phi_j - \phi_{j'})}} \simeq \frac{\hbar}{l_{\parallel} \delta K} \simeq \frac{\sqrt{\hbar}}{\delta K} e^{-\lambda_1 t}. \quad (16)$$

Because of the large number of crossings there is now little difference between \bar{M} and logarithmic averages. For $t > \tau_E + 2\tau_0$ the number of crossings becomes $N_c \simeq \delta K l_{\parallel}^2$. (The distance between almost parallel segments of $p'(x)$ is of order $1/l_{\parallel}$, and the line $p(x)$ crosses at the angle δK about $\delta K l_{\parallel} \gg 1$ segments per unit length.) This leads to saturation of the overlap at $\bar{M} \simeq \hbar$.

This completes our discussion of the intermediate regime $\hbar < \delta K < \sqrt{\hbar}$. We conclude with a brief discussion of the two other regimes. For $\delta K > \sqrt{\hbar}$ the longitudinal displacement of the packets exceeds their lengths $\Delta_{\parallel} > l_{\parallel}$. The logarithmic averages now remain

the same, but \bar{M} is changed. The dominant contributions to \bar{M} are now given by the rare events for which both Δ_{\perp} and Δ_{\parallel} vanish. This leads to $\bar{M} \simeq (\hbar/\delta K^2)e^{-\lambda_1 t}$ for $t < 2\tau_0$. (The same Lyapunov decay as in the intermediate regime, but with a much smaller prefactor.) For $2\tau_0 < t < \tau_E$ the length of each wave packet remains small, $l_{\parallel} \simeq \sqrt{\hbar}e^{\lambda t} \ll 1$, but the displacement saturates at the maximal value $\Delta_{\parallel} \simeq 1$. In this time range the average overlap has a plateau at $\bar{M} \simeq \hbar/\delta K$. Finally, for $t > \tau_E$ the decay (16) $\bar{M} \simeq (\sqrt{\hbar}/\delta K)e^{-\lambda_1 t}$ is recovered.

In the remaining regime $\delta K \ll \hbar$ we find from Eq. (6) that $M(t)$ remains close to unity for $t < \tau_E$, regardless of the initial location of the wave packet. (This also results in insensitivity to the way of averaging.) The golden-rule decay [5], with rate $\Gamma \simeq (\delta K/\hbar)^2$, sets in only after the Ehrenfest time: $\bar{M} \simeq \exp[-\Gamma(t - \tau_E)]$ for $t > \tau_E$. These results are depicted in Fig. 4. Golden-rule decay persists until the Heisenberg time $t_H \simeq 1/\hbar$ or the saturation time $\Gamma^{-1}|\ln \hbar|$, whichever is smaller. (Only the initial decay is shown in Fig. 4.) The Gaussian decay [5] sets in for $t > t_H$ provided that $\delta K < \hbar^{3/2}$.

In summary, we have shown that statistical fluctuations play a dominant role in the problem of the Loschmidt echo on time scales below the Ehrenfest time. While the decay of the squared overlap $M(t)$ of two perturbed wave packets is exponential on average, as obtained previously [4], the typical decay is double exponential. It is only after the Ehrenfest time that the main part of phase space follows the single-exponential decay of \bar{M} . The Ehrenfest time has been heavily studied in connection with the quantum-to-classical correspondence [5]. The role which this time scale plays in suppressing statistical fluctuations has not been anticipated in this large body of literature.

We acknowledge discussions with E. Bogomolny. This work was supported by the Dutch Science Foundation NWO/FOM. J.T. acknowledges support of the European Community's Human Potential Program under contract HPRN-CT-2000-00144, Nanoscale Dynamics.

-
- [1] F. Haake, *Quantum Signatures of Chaos* (Springer, Berlin, 2000).
 - [2] R. Schack and C. M. Caves, Phys. Rev. Lett. **71**, 525 (1993); Phys. Rev. E **53**, 3257, 3387 (1996).
 - [3] A. Peres, Phys. Rev. A **30**, 1610 (1984).
 - [4] R. A. Jalabert and H. M. Pastawski, Phys. Rev. Lett. **86**, 2490 (2001).
 - [5] Ph. Jacquod, P. G. Silvestrov, and C. W. J. Beenakker, Phys. Rev. E **64**, 055203(R) (2001); F. M. Cucchietti, H. M. Pastawski, D. A. Wisniacki, Phys. Rev. E **65**, 045206(R) (2002); N. Cerruti and S. Tomsovic, Phys. Rev. Lett. **88**, 054103 (2002); D. A. Wisniacki and D. Cohen, nlin.CD/0111125; F. M. Cucchietti, C. H. Lewenkopf, E. R. Mucciolo, H. M. Pastawski, and R. O. Vallejos, nlin.CD/0112015; T. Prosen and T. Seligman, nlin.CD/0201038.
 - [6] R. Ketzmerick, K. Kruse, and T. Geisel, Physica D **131**, 247 (1999).
 - [7] H. Schomerus and M. Titov, cond-mat/0204371.
 - [8] These relations between l_{\parallel} , l_{\perp} and α , β follow most easily by writing the wave function in the Wigner representation, see P. G. Silvestrov and C. W. J. Beenakker, Phys. Rev. E **65**, 035208(R) (2002).
 - [9] G. Benenti and G. Casati, quant-ph/0112060.
 - [10] T. Prosen and M. Znidaric, J. Phys. A **35**, 1455 (2002).
 - [11] B. Eckhardt, preprint.
 - [12] M. V. Berry and N. L. Balazs, J. Phys. A **12**, 625 (1979).